IEEE Access
Multidisciplinary | Rapid Review | Open Access Journal

Received November 26, 2019, accepted January 8, 2020, date of publication January 21, 2020, date of current version February 6, 2020.

Digital Object Identifier 10.1109/ACCESS.2020.2968366

Research on Earth Resistivity Measuring and Modeling of HVDC Deep-Well Grounding Electrode Sites

MAOHENG JING[1], XISHAN WEN[1], HANSHENG CAI[2], YUN TENG[1], SHANGMAO HU[2], YI ZHANG[2], LEI LAN[1], AND HAILIANG LU[1], (Member, IEEE)

[1]School of Electrical Engineering and Automation, Wuhan University, Wuhan 430072, China
[2]Electric Power Research Institute, CSG, Guangzhou 510670, China

Corresponding author: Hailiang Lu (luhailiang@whu.edu.cn)

This work was supported in part by the Major Project of China Southern Power Grid Research of HVDC Deep Well Grounding Electrode Technology and Its Application under Grant WY-KJXM-20150901, and in part by the Electric Power Research Institute of CSG.

ABSTRACT HVDC Deep-well grounding electrode covers a small area, which effectively alleviates the problem of difficulty in selecting the site of grounding electrode. Due to the small number of electrodes, each sub-electrode has to bear tens of times the current of conventional electrodes. In order to reduce the current density on the electrode, it is usually necessary to use long vertical electrodes to extend into low resistivity layers' hundreds of meters underground. Because it involves a wide range of underground depths, it is particularly important to accurately evaluate the distribution of resistivity at the electrode site for calculating the electrical parameters of deep-well grounding electrodes. In this paper, four-point method (FP), controllable source audio magnetotelluric method (CSAMT) and magnetotelluric method (MT) are proposed to analyze the conductivity structure of the shallow layer, deep layer and the vicinity of the electrode, and the earth resistivity model of deep-well grounding electrode is obtained. By comparing the on-site grounding resistance measurements of practical engineering application, it is found that the absolute error of the earth resistivity model obtained in this paper is 0.064Ω when calculating the grounding resistance of the deep-well grounding electrode. Engineering examples show that the exploration method in this paper has strong adaptability to the site, and the earth resistivity modeling method has good reliability.

INDEX TERMS HVDC deep-well grounding electrode, earth resistivity, four-point method, controlled source audio magnetotelluric method, magnetotelluric method, grounding resistance.

I. INTRODUCTION

High-voltage direct current (HVDC) power transmission systems have advantages over AC systems, such as low transmission losses, making it economical to transfer large amounts of power over distances of thousands of kilometers [1]. The entire transmission is completed in monopolar ground return or bipolar modes. The DC grounding electrode may withstand up to several kA of grounding current during the debugging of the DC transmission system or unipolar fault [2]. In order to reduce the heating and corrosion of DC grounding electrodes caused by this grounding current, conventional grounding electrodes can only be solved by increasing the number of electrodes and the occupied area [3]–[6]. Compared with traditional grounding electrodes, deep-well grounding electrodes reduce the requirements on terrain conditions and occupied area, which not only can reduce the difficulty of site selection, but also can shorten the distance between grounding electrodes and converter stations, and greatly reduce the construction cost of grounding electrode leads. At the same time, the introduction of strong current into the deep low-resistance layer has certain advantages in reducing grounding resistance and step voltage, and is an effective grounding electrode arrangement scheme [7]–[9].

However, deep-well grounding electrodes are facing problems in construction due to their large depth of burial, so they are rarely used in practical engineering. At present, only the experimental deep-well grounding electrodes were

The associate editor coordinating the review of this manuscript and approving it for publication was Amedeo Andreotti.

installed at the Swedish converter station of the Baltic Cable project [10]. However, the literature on this experiment has not been published, and no similar deep electrode project has been applied. The grounding electrode of the 533kV Cahora Bassa DC transmission project from Mozambique to South Africa is operated in parallel with four 90m long vertical electrodes with a depth of 40m. The Cantons-Comerford DC project from the United States to Canada uses six 60m vertical grounding electrodes in a circular arrangement [11]. In addition to the above mentioned projects, vertical grounding electrode is still mainly used as the resistance reduction at this stage, which is combined with horizontal grounding grid to reduce grounding resistance and step voltage.

In order to study the performance of DC grounding electrodes, many scholars have proposed various models, such as CDEGS model, unequal potential model, Finite element model (FEM) and model considering deep earth resistivity [12]–[16], [31]–[35]. References show that these methods have achieved good application effects. CDEGS software and FEM are currently the mainstream simulation methods. For grounding electrode simulations that require precise modeling, such as temperature rise calculations, the FEM is more appropriate. However, the FEM is slow in calculating large grounding electrodes and requires more computer memory.

Based on the further improvement of the theoretical model of DC grounding electrode, how to select an accurate earth resistivity parameter model of grounding electrode site is the key to improve the accuracy of grounding electrode model solution. Literature [17] investigated the potential location of India's first 800 kV, 6000 MW HVDC grounding electrode through a combination of magnetotelluric (MT) and electrical resistivity tomography (ERT) technologies. The results show that the MT can provide deep resistivity information, while the ERT can depict a detailed shallow resistivity structure for electrode design parameters. At present, there are two main methods for resistivity exploration of grounding electrode sites in DC transmission projects: electrical method and magnetic method.

Electrical method: There are many types of electrical exploration methods, and each method has its own characteristics and limitations. For example, Vertical Electric Sounding (VES) has good resolving power for both high-resistance and good-conducting layers, but due to the equivalence of the sounding curve, the response to the thin layer depends only on the conductivity-thickness (good conductance Layer) or the product of resistivity-thickness (high-resistance layer), so VES can hardly distinguish models containing high-contrast feature layers [17]. The electrical method represented by Four-point (FP) method has been widely used in the earth resistivity exploration of substations and towers in power systems [29]. FP method needs to face the problem of insufficient depth measurement caused by limited pole length in the field. In reality, it is often difficult to meet the exploration demand of the earth resistivity. In addition, the mutual inductance between leads cannot be ignored under the condition of large pole distance[18].

Magnetic method: According to the nature of field sources, magnetic exploration can be divided into natural source method and artificial source method. The magnetotelluric method (MT) in the natural source method is currently the largest depth of detection, the sounding can reach tens to hundreds of km. MT was proposed and established by Tikhonov (1950) and Cagniard (1953) [17], and has played an important role in deep earth tectonic detection, natural earthquake prediction and other fields. However, due to the use of natural field sources, the MT method has weak signals and random defects, and the observation accuracy and resolution are low. Controlled Source Audio-frequency Magnetotelluric (CSAMT) is an artificial source frequency domain electromagnetic detection method proposed by trangway and Goldtein in the early 1970s [18], the artificial field source is used instead of the natural field source, and the observation method of MT is used to overcome the short-comings of the randomness of the MT field source, and the signal strength is also greatly improved. It has been widely used in the fields of metal ore [19]–[21], geothermal [22]–[23], and hydrological environment [24]. According to skin effect, its sounding is generally in the range of tens of meters to 3km. Although the CSAMT can overcome the influence of interference, the biggest problem with the magnetic method is that it cannot accurately measured the ground resistivity distribution within a few meters of the shallow layer. However, the shallow resistivity distribution will cause the deviation of deep resistivity data inversion, which needs to be overcome in the field use of geodetic resistivity.

To sum up, the current resistivity exploration for DC grounding electrode sites is relatively complex, and the single method is difficult to fully meet the requirements of the DC deep-well grounding electrode sites for earth resistivity exploration. The model of earth resistivity distribution is very important to evaluate whether the grounding electrode can operate safely. However, the conductivity structure depth near the electrode in the literature is far from enough for the deep-well grounding electrode.

Although deep-well DC grounding electrode has many advantages, there is no successful experience for reference at present. In order to accurately evaluate the grounding resistance of the deep-well grounding electrode, this paper based on the FP, CSAMT and MT methods to measure the earth resistivity of the actual deep-well grounding electrode site, analyzed the conductivity structure of the shallow layer, deep layer and the electrode nearby, and proposed the earth resistivity model to calculate the grounding resistance of deep-well grounding electrodes. By comparing the field measurement data of actual projects, it is found that the absolute error of the earth resistivity model in calculating the grounding resistance of deep-well grounding electrode is 0.064Ω. It is proved that the earth resistivity model obtained in this paper has good reliability.

TABLE 1. Nomenclature.

Symbol	Meaning
Z	Impedance
ρ	Apparent resistivity,
T	Period
E_x	Electric field in x direction
E_y	Electric field in y direction
D	Distance between two non-polarized electrodes in same direction
Hx	Magnetic field in x direction
H_y	Magnetic field in y direction
f	Frequency
ρ_{TM}	Apparent resistivity of Transverse Magnetic mode
ρ_{TE}	Apparent resistivity of Transverse Electric mode

TABLE 2. Main parameters of deep-well grounding electrode.

Rated ground current	3125A
Maximum Over Load Current	3487A
Bipolar unbalanced ground current	10A
Max continuous operating current and time (Unipolar)	3125A/24h
Polarity	Cathode/anode
Design Life	35 years

II. INFLUENCE OF EARTH RESISTIVITY ON DEEP-WELL GROUNDING ELECTRODE

The advantages of deep-well grounding electrode is that it covers a small area, lower surface electric potential and gradient, and lower the risk of corrosion caused by current exchange between soil and buried facilities [2]. However, this requires that the earth structure has a relatively high resistivity in the shallow layer and the deeper earth structure has very low resistivity. The earth structure near the grounding electrode may have great influence on its grounding resistance. This section will focus on the influence of different earth stratification near the electrode on its grounding resistance.

A. DESIGN PARAMETERS OF DEEP-WELLGROUNDING ELECTRODE

China Southern Power Grid Research Institute adopts the idea of co-location construction of deep-well grounding electrodes and vertical elliptical ring grounding electrodes. There are 52 shallow-buried vertical grounding electrodes in the periphery. The purpose of this construction is to prevent deep-well grounding electrodes from malfunctioning and can be switched to conventional grounding electrodes. The deep-well grounding electrodes are 3 deep wells with a depth of 1,000 m distributed in a regular triangle, and the electrode spacing is 100m. The inner diameter of the wellhead is 610mm, and the diameter of the retaining sleeve is 340 mm. Oil coke is filled around the feed electrode of the protection sleeve. The main design parameters of deep-well grounding electrodes are shown in Table 2 and Fig 1.

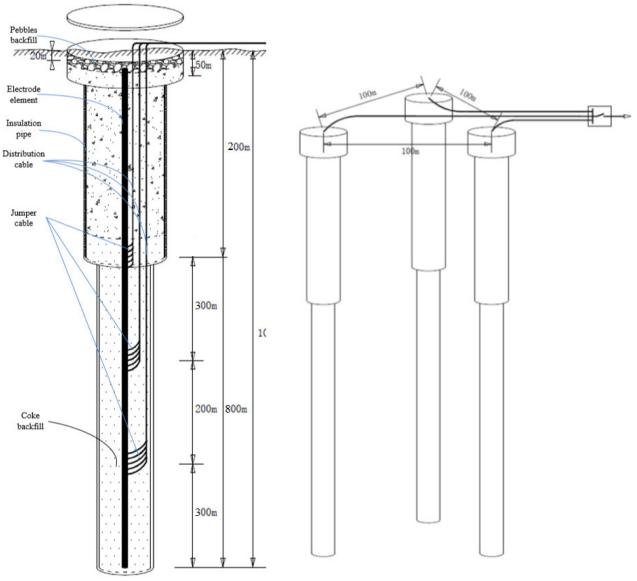

FIGURE 1. Schematic diagram of 1000m deep-well grounding electrode.

TABLE 3. 3-Layer earth model.

No. of strata (layer)	Layer thickness (m)	Resistivity (Ω.m)
1	100	2000
2	900	300
3	Infinite	200

TABLE 4. 5-Layer earth model.

No. of strata (layer)	Layer thickness (m)	Resistivity (Ω.m)
1	100	2000
2	200	500
3	300	150
4	400	300
5	Infinite	200

B. SIMULATION CALCULATION OF DEEP-WELL GROUNDING ELECTRODE

Because the earth resistivity distribution involved in deep-well grounding electrodes is not encountered by conventional grounding electrodes, it is very important to accurately calculate the grounding resistance before building such large grounding electrodes. The size of grounding resistance directly determines whether it can operate safely. Because the FEM is slow to simulate 3D large-scale grounding electrodes, this paper uses the grounding system commercial software CDEGS for simulation. Its advantage is that it simplifies the electrodes model and speeds up the calculation.

According to the special earth resistivity structure of the deep-well grounding electrode, the grounding resistance of deep-well grounding electrode under three different earth models is calculated and compared.

From the calculation results in Table 6, it can be seen that for a 1000m deep-well grounding electrode, changing the size of layered resistivity near the electrode has a great influence

TABLE 5. 5-Layer earth model with different parameters.

No. of strata (layer)	Layer thickness (m)	Resistivity (Ω.m)
1	100	2000
2	200	600
3	300	50
4	400	250
5	Infinite	200

TABLE 6. Comparison of grounding resistance for changing soil structure near electrode.

	Soil structure	Grounding resistance (Ω)
Parallel connection of three electrodes	Table III	0.4804
	Table IV	0.3892
	Table V	0.1981

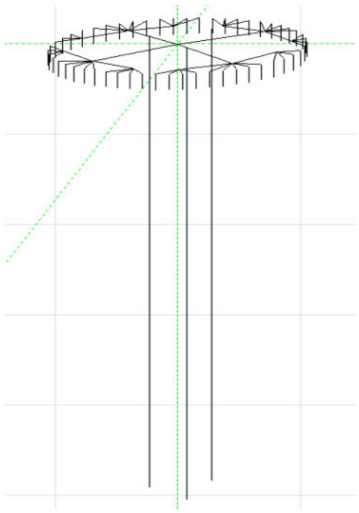

FIGURE 2. CDEGS model of deep-well grounding electrode.

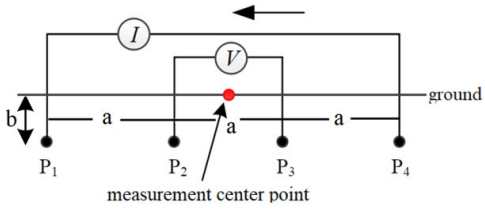

FIGURE 3. Schematic diagram of induced polarization method wiring.

on the calculation of grounding resistance, so it is particularly important to accurately measure the earth resistivity of electrode burial depth. At present, the commonly used FP method will face the problem of being unable to penetrate through the high resistivity layer when measuring areas with high shallow resistivity, and the depth measurement is insufficient. MT method can reach hundreds of km in depth due to its advantages in monitoring low frequency bands. The natural source method has poor anti-interference ability. The biggest problem is that it cannot accurately obtain the earth resistivity distribution in the shallow and middle layers. To sum up, this paper adopts a new idea to solve the problem of DC deep-well grounding electrode site resistivity survey.

III. HVDC DEEP-WELL GROUNDING ELECTRODE SITE RESISTIVITY SURVEY

A. EXPLORATION TARGETS

The depth of deep-well grounding electrode site may exceed 1000m. According to the research results of literature [27], accurate earth resistivity measurement within 10 times the size of DC electrode is the basis for grounding electrode design. In other words, the earth resistivity in the 10km depths of the electrode site is closely related to the grounding electrode parameters.

B. OVERALL THINKING OF EXPLORATION METHODS

The earth resistivity measurement of the grounding electrode site includes electrical and magnetic method. The principles of three methods are different from each other. The data processing and inversion algorithms of electrical and electromagnetic methods are very different, so there is no common theoretical basis for these methods, and joint inversion is not currently available. The three methods are not a combination of principles, but are combined from an application perspective to adapt to their respective sounding range. This paper uses FP method to measure the accuracy of shallow layer data, CSAMT method's anti-interference ability and MT method's large depth measurement ability to effectively cover the earth resistivity from the surface to the depth of tens of kilometers underground. CSAMT method is used to measure the underground conductivity structure near the electrode position.

C. FP METHOD

The FP method is a method for measuring the apparent resistivity of large volumes of undisturbed soil. Four auxiliary probes are installed underground, all at depth b, separated by a (in a straight line). The test current I is passed between the two external probes, and the potential V between the two internal probes is measured with a voltmeter [29]. This paper uses the wenner arrangement in the FP method. The schematic diagram for the FP is given in Fig. 2, p_1 and p_4 are current electrodes, p_2 and p_3 are voltage electrodes, the measurement steps are as follows:

(1) Measurement location is investigated to determine the center point of measurement.

(2) Maintain the position of the measuring center point unchanged, and use the north-south direction (or whichever direction) wiring to measure the polar distance a by the induced polarization method.

(3) Keep the position of the measurement center point unchanged, conduct the same measurement in the east-west direction (or perpendicular to the previous measurement direction) wiring mode and polar distance arrangement,

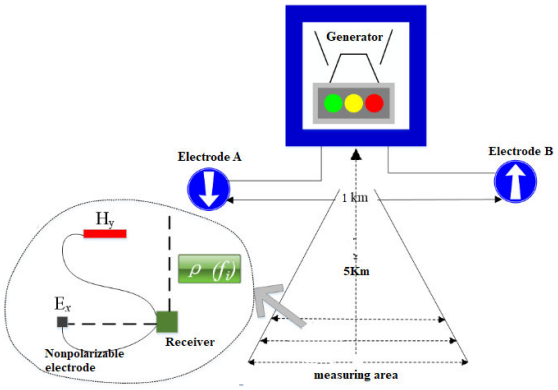

FIGURE 4. The schematic diagram of CSAMT method.

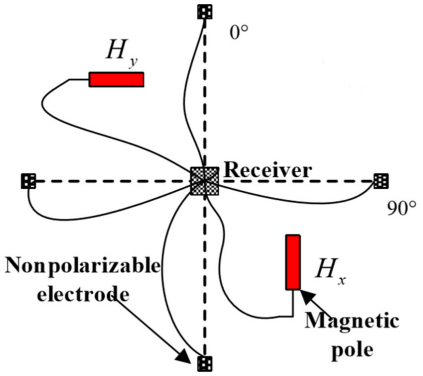

FIGURE 5. The schematic diagram of MT method.

and observe the difference of apparent resistivity in the two directions.

(4) Carry out one-dimensional inversion of soil model after completing the polar distance arrangement of required groups.

For one-dimensional inversion can be derived by the method of references [28], and will not be repeated here. The biggest disadvantage of FP method is that the depth measurement is deeply influenced by the polar distance. When the grounding electrode size is over 1km, to obtain 10 times the depth of the grounding electrode size, the electrode distance of the FP method should reach at least 10km. This is impossible to do in reality and different methods need to be introduced to fill in the deficiency of FP method.

D. CSAMT METHOD

CSAMT is an artificial source frequency sounding method developed on the basis of AMT. The method mainly uses an artificial field source of an electrical source, the equatorial dipole device performs the measurement, and simultaneously observes the electric field horizontal component Ex parallel to the field source and the magnetic field horizontal component Hy orthogonal to the field source. The Cagniard impedance phase is calculated using the electric field phase and the magnetic field. The resistivity parameters were calculated by inversion of impedance resistivity and impedance phase, and the inversion resistivity is used for geological inference interpretation.

Fig. 4 shows the measurement scheme of CSAMT. The measurement process of CSAMT method is as follows:

(1) Arrange the transmitter and source A and B, and arrange the electrodes and magnetic poles of CSAMT at the measuring point.

(2) Measure the data of the apparent resistivity corresponding to the measured point.

(3) Determine the validity of the measured data from the electric field-magnetic field correlation and decide whether to make repeated measurements.

(4) Perform a one-dimensional inversion of a single point. CSAMT uses the Caginiard resistivity to reflect the characteristics of soil current divergence. The ratio of the two horizontal orthogonal electromagnetic fields (E_x, H_y) observed on the ground is defined as the Caginiard resistivity, its physical meaning and unit are the same as resistivity:

$$Z = \frac{E_x}{H_y} \tag{1}$$

Z is the impedance and the resistivity is given by:

$$\rho = 0.2 \cdot T \cdot (|Z|)^2 \tag{2}$$

where T is period, ρ is the apparent resistivity.

(5) The sounding is determined jointly by the inversion result and the measurement data, and it is judged by the sounding whether the measurement of steps 2-4 is repeated.

(6) Move the measuring point and repeat steps 2-5 until the measurement of all measuring points is completed.

The biggest disadvantage of CSAMT method is that the sounding is deeply influenced by frequency, and it is difficult to obtain shallow earth resistivity when the buried depth of grounding electrode is only a few meters. CSAMT sounding depends on the resistivity of the formation. If the resistivity is larger, the measured depth will be deeper, and if it is low resistivity, it will be shallow. In general, CSAMT can reach 3km.

E. MT METHOD

MT method is a typical method of magnetic exploration and is also widely used in geological survey and mineral exploration. The MT measurement scheme is actually similar to the CSAMT method. The difference between the two is the difference in the measurement frequency band and the difference in the field source. The MT method mainly observes the orthogonal components of the natural earth electric field and magnetic field.

Fig. 5 shows the measurement scheme of MT. The measurement process of MT method is as follows:

(1) The electrodes and magnetic poles of the MT method are arranged at the measurement center point, and the non-polarized electrode is arranged in the four directions of southeast and northwest respectively, the four electrodes are

centered on the receiver, the electrode distances in the east, west, north and south directions are D, potential differences V_x and V_y in xy direction are measured, and magnetic poles are arranged in x and y two directions of the second and fourth quadrants shown in Fig. 5 to measure the two components H_x and H_y and of the magnetic field respectively.

The electric fields in the x and y directions measured by the non-polarized electrode are calculated as follows:

$$E_x = \frac{V_x}{D} \tag{3}$$

$$E_y = \frac{V_y}{D} \tag{4}$$

Where E_x is the electric field in the x direction, E_y is the electric field in the y direction, D is the distance between two non-polarized electrodes in the same direction.

(2) Monitoring electric field and magnetic field data in a period of time, extracting electric field and magnetic field in a frequency range, and calculating the apparent resistivity of the TM and TE modes:

$$\rho_{TM} = \frac{E_x}{H_y} \cdot \frac{1}{5 \cdot f} \tag{5}$$

$$\rho_{TE} = \frac{E_y}{H_x} \cdot \frac{1}{5 \cdot f} \tag{6}$$

where ρ_{TM} is the apparent resistivity of TM (Transverse Magnetic) mode, ρ_{TE} is the apparent resistivity of TE (Transverse Electric) mode.

(3) Taking out all frequency points, and performing one-dimensional inversion of the geodetic model.

(4) The inversion result and the measurement data are used to jointly determine the sounding, and whether the requirements are met or not is judged by the sounding. If not, the measurements in steps 2 to 4 are repeated.

IV. RESULTS

In this paper, FP, CSAMT and MT method are used to collect field data for geodetic resistivity testing. Three kinds of main instruments and equipment are used, which are DET2/2 multi-function DC electric instrument (FP), GDP-32 series multifunctional electrical method instrument system (CSAMT) and V5-2000 magnetotelluric sounding instrument (MT). The earth resistivity measurement is divided into three sections with different depths, FP is used to measure the earth resistivity of 0-100m, CSAMT is used to measure the earth resistivity of 100-3km, The MT method is used to measure the earth resistivity distribution below 3km. A schematic diagram of the earth resistivity field measurement is shown in Fig. 6. Due to the limitations of on-site measurement conditions, the four-pole method uses three vertical and one horizontal methods (blue lines F1-F4) to avoid areas where vertical grounding has been buried. The CSAMT method adopts a five-line arrangement, which is L2-L6 (yellow line in the figure). L1 gives up the measurement because it passes through the residence and grave of the local residents, which is not shown in Fig. 6. L2 is 70m away from L3, and L3 to L6 are separated by 50m. According to the on-site interference conditions, the MT method has four measuring points, which are M1-M4.

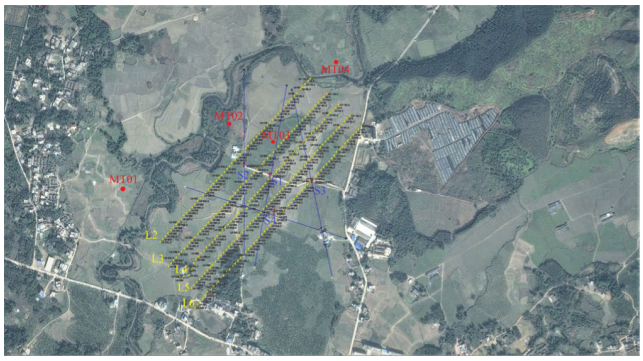

FIGURE 6. Schematic diagram of the measurement points at deep-well grounding electrode site.

TABLE 7. Soil resistivity model of FP method.

Vertical direction			Horizontal direction	
Depth (m)	Resistivity (Ω·m)		Depth (m)	Resistivity (Ω·m)
0-20	Maximum	305	0-20	248
	average	265		
	Minimum	225		
20-50	Maximum	520	20-50	505
	average	484		
	Minimum	448		
50-100	Maximum	3120	50~150	2770
	average	2870		
	Minimum	2620		

By inverting the measurement data of the FP method, it can be concluded that the shallow layer of the deep-well grounding electrode site is roughly divided into three layers. The FP method showed that the soil resistivity in the two directions was slightly different. The surface resistivity was basically the same, roughly 240-260Ω·m. After the depth was more than 20m, the resistivity in the horizontal was slightly higher, as shown in the table 7.

CSAMT tests the earth resistivity at a depth of about 100m-3km. For the 5 survey lines, the commercial inversion software (SCS2D) published by Zonge Company of the United States was adopted to perform two-dimensional inversion of the preprocessed CSAMT data. Then, MODSET software is used to convert the model resistivity section generated by inversion of the above program into Surfer grid file, and the converted apparent resistivity section is edited and drawn. Two-dimensional inversion is carried out on the five survey lines, with the abscissa as the sounding point and the ordinate as the inversion depth. The corresponding relationship between the earth resistivity at each measuring point along the depth direction can be seen in the cross-section diagram.

Because the scalar mode is highly efficient, CSAMT mainly uses the TM mode, so only the inversion results

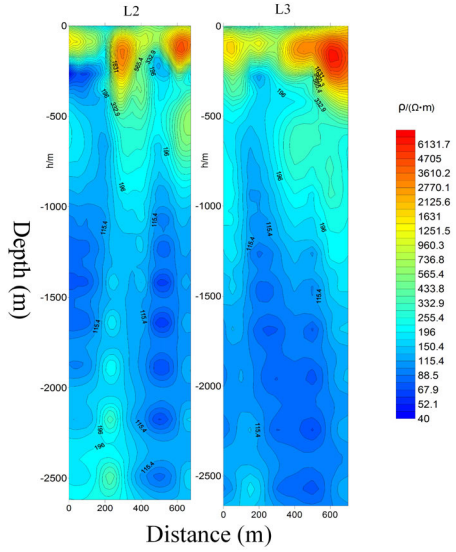

(a)

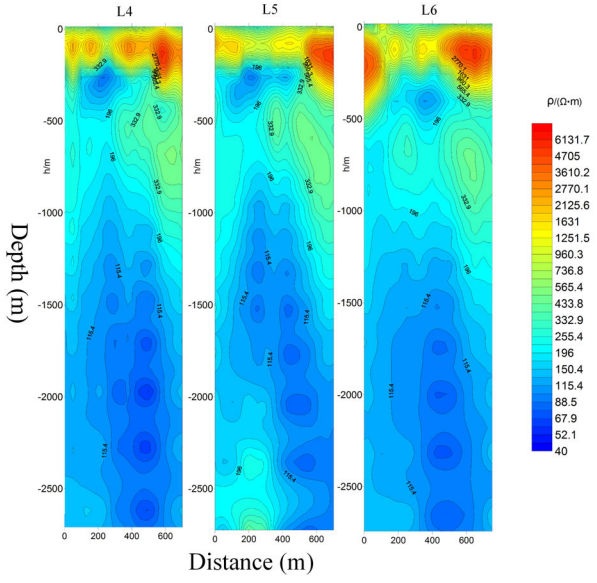

(b)

FIGURE 7. Inverted 2-D resistivity section of CSAMT (L2-L6) (a) Line L2-L3 (b) Line L4-L6.

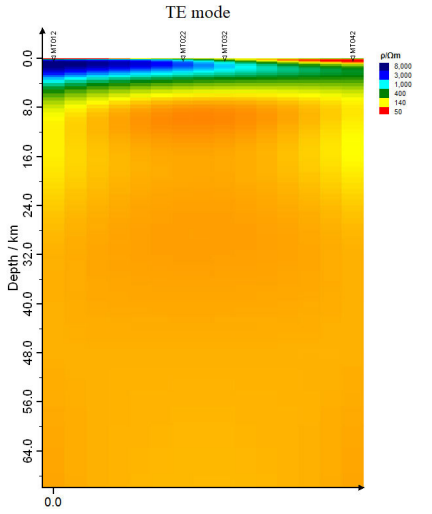

FIGURE 8. TE mode resistivity inversion results (MT).

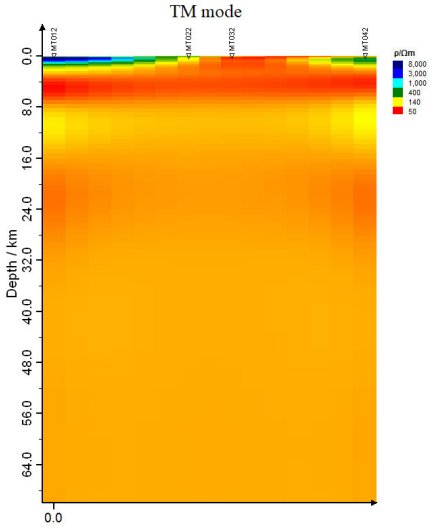

FIGURE 9. TM mode resistivity inversion results (MT).

of the TM mode are available. It can be seen from the inversion results of Fig. 6 that the resistivity distributions of the five cross-sections are roughly the same, and all of them show a high-resistance layer of about 300m from the surface to the ground, and a low-resistance layer of about 300m to 3000m. Since the conductivity distribution near the electrode is critical for calculating the grounding resistance of the deep-well grounding electrode, the weighted average of the large original data is obtained, and the earth resistivity with the depth of 100-3km can be divided into five layers. The first layer is from a depth of 100 m to about 200 m, and the average resistivity is 2770Ω·m. The second layer is about 200 m to 300 m in depth, and the average resistivity is 150Ω·m. The third layer is about 300m to 700m in depth, and the average resistivity is 255Ω·m. The depth is about 700m to 1200m, and the fourth layer has an average resistivity of 115Ω·m. The depth is about 1200m to 3000m, and the fifth layer has an average resistivity of 67Ω·m.

The MT method measured the earth resistivity of the formation below 3km. Because the industrial high-frequency current or AC transmission circuit interferes with the MT method measurement seriously, the measurement point needs to be more than 1km away from the transmission line, so it is difficult to measure the MT measurement point in a straight line. Since there are only four MT sounding points and they are not on a straight line, it is not possible to arrange survey lines according to real coordinates for 2D inversion. Therefore, in the two-dimensional inversion result diagram, the abscissa includes four sounding points of MT021, MT022,

TABLE 8. Earth resistivity model of MT method.

TE mode		TM mode	
Depth (m)	Weighted average resistivity (Ω·m)	Depth (m)	Weighted average resistivity (Ω·m)
0~200	173.04	0~500	994.66
200~3k	2787.04	500~7k	77.60
3k~6k	287.80	7k~14k	114.92
6k~68k	106.09	14k~68k	96.01

TABLE 9. Earth resistivity model of deep-well grounding electrode.

Layer	Thickness (m)	Resistivity (Ω·m)
1	20	248
2	50	484
3	130	2770
4	100	150
5	408	255
6	500	115
7	1792	67
8	4000	78
9	7000	115
10	Infinite	79

MT023 and MT024, the ordinate is the inversion depth, and the corresponding relationship between the earth resistivity at each measuring point along the depth direction can be seen in the cross-section diagram below.

In the MT data processing, a large amount of data is also subjected to a weighted average calculation. From the above TE mode inversion results, the earth resistivity can be roughly divided into 4 layers. From the surface to a depth of about 200m, the first layer has the average resistivity of 173.04Ω·m. The second layer is about 200m deep to about 3000m deep, with the average resistivity of 2787.04Ω·m. The third layer is about 3000m deep to 6000m deep, with the average resistivity of 287.80Ω·m. The fourth layer is about 6000m deep to 67898m deep, with an average resistivity of 106.09Ω·m.

In the TM model inversion results, the Earth resistivity can also be roughly divided into 4 layers. The first layer is about 500m from the surface to the depth, with the average resistivity of 994.66Ω·m. The second layer has a depth of about 500m to 70,000 m, the average resistivity is 77.60Ω·m. The third layer is about 7000m deep to 14000m deep, with an average resistivity of 114.92Ω·m. The fourth layer is about 14000m deep to 67898m deep, with the average resistivity of 96.01Ω·m.

Based on the test data, the soil model was inverted and fitted. Finally, we obtained the grounding resistivity layered model of the deep-well grounding electrode, as shown in Table 9.

V. GROUNDING RESISTANCE MEASUREMENT AND SIMULATION VERIFICATION OF DEEP-WELL GROUNDING ELECTRODE

A. MEASUREMENT METHOD FOR GROUNDING RESISTANCE OF DEEP-WELL GROUNDING ELECTRODE

In order to verify the accuracy of the earth resistivity model obtained by the above-mentioned three methods,

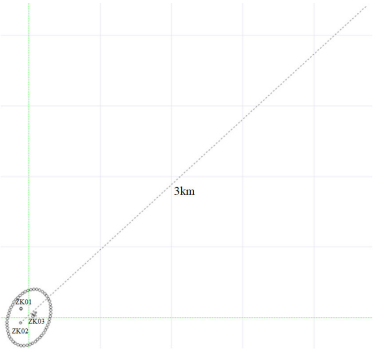

FIGURE 10. CDEGS model of potential distribution curve of grounding electrode.

the deep-well grounding electrode current injection experiment was carried out. To measure the grounding resistance of the deep-well grounding electrode, a certain current must be injected into the grounding electrode first, which requires setting a current electrode that can provide a current loop. However, in order to measure the ground potential rise of the deep-well grounding electrode, it is necessary to set a voltage electrode at zero potential. In fact, since the voltage electrode cannot be arranged at the true zero potential at infinity, and the existence of the current electrode will distort the current field in the ground and affect the potential distribution on the ground, there may be errors in the measurement of the grounding resistance. Reasonable arrangement of the current pole and the voltage pole is the key to the measurement of the grounding resistance.

According to IEEE Std 81^{TM}-2012[29], the recommended potential drop method is used to measure the grounding resistance of deep-well grounding electrodes, which requires determining the range of influence of the deep well grounding electrodes. In order to reduce the influence of the auxiliary current electrode on the surface potential distribution generated by the deep-well grounding electrode, the current electrode should be set outside the influence range of the deep-well grounding electrode.

The deep-well grounding electrode was modeled and analyzed using the MALZ module of the CDEGS software, as shown in Fig. 10. Taking the ZK02 electrode as an example, a DC current of 100A is injected into the grounding electrode. The dotted line in the figure is the observation line and is located at the surface of the ground. Considering the site topography, the center of the elliptical grounding electrode is now taken as the origin of coordinates, and the observation line is about 3 kilometers. The potential distribution curve is shown in Fig. 11.

The calculation results show that the conductor ground potential at the current injection point rises to about 28.38V. It can be seen from Fig. 11 that the ground potential at 1986m from the deep-well grounding electrode is about 1.419V, which is less than 5% of the ZK02 electrode potential. If it is considered that the ground potential rise below 5% of the ground potential rise of the current injection conductor

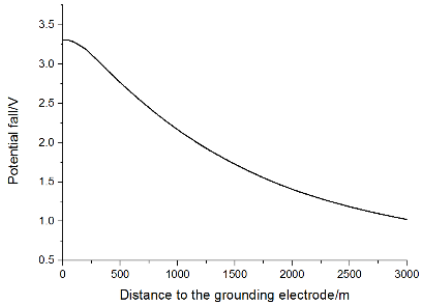

FIGURE 11. Potential distribution curve of ZK02 electrode.

section is outside the action range of the ZK02, the influence range radius of the deep-well grounding electrode of ZK02 is about 1703.98m. Thus, the linear distance of the current electrode from the grounding electrode should be at least 1986m. Considering comprehensively, the current electrode distance is 3,000 m to measure the grounding resistance of the deep-well grounding electrode.

However, the auxiliary current electrode moves the infinite zero potential point to the middle of the current electrode connection. In other words, the auxiliary current electrode causes the voltage difference between the ground electrode and the zero potential point to be smaller than the voltage difference when the auxiliary current electrode is not provided, and even if the voltage electrode is set at the zero potential point, the measured ground resistance value is still small. In order to compensate for the error caused by the current electrode, it is necessary to shift the voltage point to the right. Based on the idea of the literature [30], the voltage electrode compensation point is about 1162m. That is, the linear length of the voltage line is about 39.4% of the linear length of the current line.

B. COMPARATIVE ANALYSIS OF GROUNDING RESISTANCE MEASUREMENT RESULTS

The auxiliary current electrode and voltage electrode are arranged based on the simulation calculation results in Fig. 10. The experiment uses DC power supply as the applied current source, and the distance between current electrode C and center point is 3078.16m. The measurement principle diagram is shown in Fig. 12. The voltage electrode is placed at P, and the distance between voltage electrode P and center is 1196.28m. The voltage is measured at the end of the drain cable of the deep-well grounding electrode.

The ammeter and voltmeter used in the measurement are F175C digital multimeters produced by Fluke. The voltage range is 0.1mV-1000V, the accuracy is ± 0.15%, the current range is 0.01mA-10A, and the accuracy is ±1.0%. The grounding resistance measurement results of three deep-well grounding electrodes connected in parallel are shown in Table 10. The value of grounding resistance in table 10 is calculated. In fact, the significant digits of the measured current are only 3 digits, so the ground resistance should be only 3 digits, and 4 digits are only the calculation

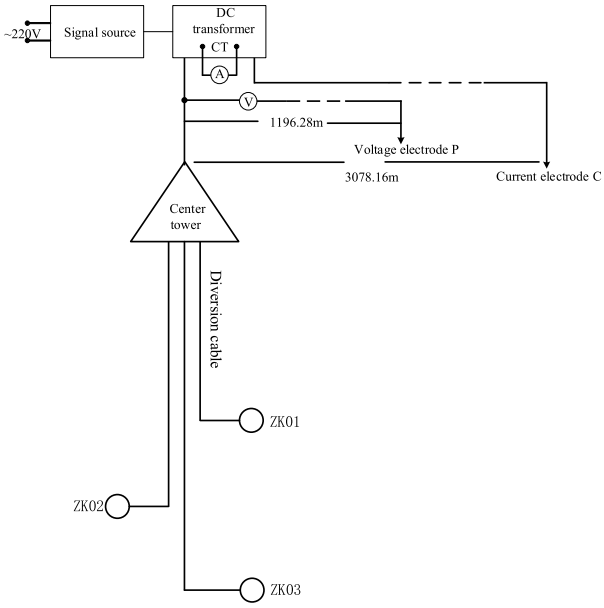

FIGURE 12. Wiring diagram of grounding resistance measurement (three-pole method).

TABLE 10. Measurement results of deep-well grounding electrodes.

Loop voltage (V)	Injection current (A)	Background noise voltage (V)	Measured voltage (V)	Calculated ground resistance (Ω)	Actual ground resistance (Ω)
416.5	5.481	-0.008	0.947	0.1743	0.174
724.5	9.552	-0.008	1.655	0.1741	

TABLE 11. CDEGS simulation results.

Electrode P voltage (V)	Injection current (A)	Grounding resistance (Ω)
23.85V	100	0.238

result. As can be seen from the table, the actual grounding resistance of three deep-well grounding electrodes is 0.174Ω.

Finally, using the earth resistivity model of table 9, the grounding resistance of the three deep-well grounding electrode in parallel operation was calculated by CDEGS to be about 0.238Ω. Since the grounding resistance of the deep-well grounding electrode is very small, we use absolute error to explain the results of the simulation and actual measurements. The absolute error is 0.064Ω compared to the actual measurement. The reliability of the earth resistivity model obtained in this paper is proved by the measurement results of the grounding resistance.

VI. CONCLUSION

In this paper, the site of the world's first HVDC grounding electrode with a buried depth of 1,000 m is studied. The research results show that the measurement method in this paper is very useful for site selection of large DC deep-well grounding electrode. Through the comparison and

analysis with the grounding resistance measurement results, the following conclusions are drawn:

1) In view of the current FP method with insufficient sounding and the problem of MT method being susceptible to interference, this paper proposes a comprehensive method of measuring the earth resistivity of deep-well grounding electrode by using FP, CSAMT and MT methods, which can more effectively cover the depth of tens of kilometers from the surface of the deep-well grounding electrode site to the underground.
2) Through inversion and analysis of the results of various measurement methods, the earth resistivity model of deep-well grounding electrode is obtained by integrating the measurement accuracy of FP shallow layer, the measurement depth of MT and the detailed conductivity structure of CSAMT near the electrode.
3) The measurement of the grounding resistance of the actual deep-well grounding pole engineering was carried out. The comparison experiment and simulation results show that the absolute error of the earth resistivity model proposed in this paper is 0.064Ω when calculating the grounding resistance of the deep-well grounding electrode. It is proved that the earth resistivity model has good reliability.

REFERENCES

[1] M. Marzinotto, G. Mazzanti, and M. Nervi, "Ground/sea return with electrode systems for HVDC transmission," *Int. J. Electr. Power Energy Syst.*, vol. 100, pp. 222–230, Sep. 2018.

[2] CIGRÉ Working Group, WGB4.61. *General Guidelines for HVDC Electrode Design*. Paris, France: CIGRE, 2017.

[3] Z. Wangjun, "Grounding electrode of HVDC transmission," in *High Voltage Direct Current Transmission Engineering Technology*, 2nd ed. Beijing, China: China Electric Power Press, 2010, ch. 13, pp. 374–432.

[4] L. Bing, S. Jian, H. Shangmao, and Z. Ran, "New research progress of HVDC transmission technology in China southern power grid corporation," in *Proc. Int. Conf. High Voltage Eng. Appl.*, New York, NY, USA, Sep. 2016, pp. 1–5.

[5] H. Jinliang and Z. Rong, "Grounding technology of HVDC transmission," in *Grounding Technology of Power System*, 1st ed. Beijing, China: Science Press, 2007, ch. 9, pp. 312–364.

[6] B. Wang, Y. H. Wang, L. J. Ding, P. Xiong, X. Y. Li. "Summary of HVDC grounding electrode and related issues," in *Proc. CSU-EPSA*, vol. 24, 2012, pp. 66–72.

[7] J. He, G. Yu, J. Yuan, R. Zeng, B. Zhang, J. Zou, and Z. Guan, "Decreasing grounding resistance of substation by deep-ground-well method," *IEEE Trans. Power Del.*, vol. 20, no. 2, pp. 738–744, Apr. 2005.

[8] Y. Teng, X. Wen, H. Cai, L. Jia, G. Liu, S. Hu, and H. Lu, "Analysis on structural parameters and electrical performance of dc deep well grounding electrode," *J. Eng.*, vol. 2019, no. 16, pp. 2366–2370, Mar. 2019.

[9] X.-S. Wen, Y. Teng, H.-S. Cai, S.-M. Hu, M.-H. Jing, Y. Zhang, H. Mei, L. Lan, and H.-L. Lu, "Experimental study on gas evolution characteristics of DC deep well grounding electrodes," *IEEE Access*, vol. 7, pp. 57450–57458, 2019.

[10] B. Arnlov, "HVDC 2000-a new generation of high-voltage DC converter stations," *Fuel Energy Abstr.*, vol. 4, no. 3, p. 273, 1996.

[11] CIGRÉ Working Group, 14.21- TF2, *General Guidelines for the Design of Ground Electrodes for HVDC Links*. Paris, France: CIGRE, 2007.

[12] F. Dawalibi and N. Barbeito, "Measurements and computations of the performance of grounding systems buried in multilayer soils," *IEEE Trans. Power Del.*, vol. 6, no. 4, pp. 1483–1490, Oct. 1991.

[13] J. Ma and F. P. Dawalibi, "Analysis of grounding systems in soils with finite volumes of different resistivities," *IEEE Power Eng. Rev.*, vol. 22, no. 3, pp. 63–64, Apr. 2002.

[14] B. Zhang, R. Zeng, J. He, J. Zhao, X. Li, Q. Wang, and X. Cui, "Numerical analysis of potential distribution between ground electrodes of HVDC system considering the effect of deep earth layers," *IET Gener. Transm. Distrib.*, vol. 2, no. 2, p. 185, 2008.

[15] W. Li, Z. Pan, H. Lu, X. Chen, L. Zhang, and X. Wen, "Influence of deep earth resistivity on HVDC ground-return currents distribution," *IEEE Trans. Power Del.*, vol. 32, no. 4, pp. 1844–1851, Aug. 2017.

[16] R. D. Southey, M. Siahrang, S. Fortin, and F. P. Dawalibi, "Using fall-of-potential measurements to improve deep soil resistivity estimates," *IEEE Trans. Ind. Appl.*, vol. 51, no. 6, pp. 5023–5029, Nov. 2015.

[17] A. Manglik, S. Verma, D. Muralidharan, and R. Sasmal, "Electrical and electromagnetic investigations for HVDC ground electrode sites in India," *Phys. Chem. Earth, Parts A/B/C*, vol. 36, no. 16, pp. 1405–1411, Jan. 2011.

[18] M. Jing, X. Wen, Z. Pan, H. Lu, H. Cai, S. Hu, G. Liu, and L. Jia, "The research on new type of Earth resistivity exploring method for HVDC deep-well Earth electrode," in *Proc. IEEE Int. Conf. High Voltage Eng. Appl. (ICHVE),* ATHENS, Greece, Sep. 2018, pp. 1–4.

[19] L. Cagniard, "Basic theory of the magnetotelluric method of geophysical prospecting," *Geophysics*, vol. 18, no. 3, pp. 605–635, 1953.

[20] M. A. Goldstein and D. W. Strangway, "Audio-frequency magnetotellurics with a grounded electric dipole source," *Geophysics*, vol. 40, no. 1, pp. 669–683, 1975.

[21] K. Okada, "Geophysical exploration at Hishikari gold mine, Kagoshima, Japan," *Leading Edge*, vol. 19, no. 7, pp. 744–750, 2000.

[22] G. Nimeck and R. Koch, "A progressive geophysical exploration strategy at the Shea Creek uranium deposit," *Leading Edge*, vol. 27, no. 1, pp. 52–63, 2008.

[23] D. E. Boerner, J. A. Wright, and J. G. Thurlow, "Tensor CSAMT studies at the Buchans mine in central Newfoundland," *Geophysics*, vol. 58, no. 1, pp. 12–19, 1993.

[24] N. Carlson, K. Zonge, G. Ring, and M. Rex, "Fluid-flow mapping at a copper leaching operation in Arizona," *Leading Edge*, vol. 19, no. 7, pp. 752–755, 2000.

[25] P. E. Wannamaker, "Tensor CSAMT survey over the sulphur springs thermal area, Valles Caldera, New Mexico, United States of America, Part I: Implications for structure of the western Caldera," *Geophysics*, vol. 62, no. 4, pp. 451–465, 1997.

[26] M. J. Unsworth, X. Lu, and M. D. Watts, "CSAMT exploration at Sellafield: Characterization of a potential radioactive waste disposal site," *Geophysics*, vol. 65, no. 7, pp. 1070–1079, 2000.

[27] *Technical Code for Design of HVDC Earth Return Operation System*, Standard DL/T 5224-2014, Ministry of Construction, Peoples's Republic of China, China Electric Power Press, Beijing, China, (in Chinese), 2014.

[28] B. Zhang, X. Cui, L. Li, and J. He, "Parameter estimation of horizontal multilayer Earth by complex image method," *IEEE Trans. Power Del.*, vol. 20, no. 2, pp. 1394–1401, Apr. 2005.

[29] *IEEE Guide for Measuring Earth Resistivity, Ground Impedance, and Earth Surface Potentials of a Grounding System*, IEEE Standard 81-2012 (Revision of IEEE Std 81-1983), Dec. 2012, pp. 1–86.

[30] H. Shanghao, "Manual wiring measurement of DC deep well grounding resistance," in *Proc. IEEE Int. Conf. High Voltage Eng. Appl. (ICHVE)*, ATHENS, Greece, Sep. 2018, pp. 1–4.

[31] J. Guemes and F. Hernando, "Method for calculating the ground resistance of grounding grids using FEM," *IEEE Trans. Power Del.*, vol. 19, no. 2, pp. 595–600, Apr. 2004.

[32] S. Georges and F. Slaoui, "Modelling and simulation of heat dissipation due to HVDC ground electrodes using the finite element method," in *Proc. IEEE Innov. Smart Grid Technol.-Asia (ISGT ASIA)*, May 2014, pp. 476–480.

[33] Z. Zhang, Y. Dan, J. Zou, G. Liu, C. Gao, and Y. Li, "Research on discharging current distribution of grounding electrodes," *IEEE Access*, vol. 7, pp. 59287–59298, 2019.

[34] J. Li, T. Yuan, Q. Yang, W. Sima, C. Sun, and M. Zahn, "Numerical and experimental investigation of grounding electrode impulse-current dispersal regularity considering the transient ionization phenomenon," *IEEE Trans. Power Del.*, vol. 26, no. 4, pp. 2647–2658, Oct. 2011.

[35] W. Sima, B. Zhu, T. Yuan, Q. Yang, and J. Wang, "Finite-element model of the grounding electrode impulse characteristics in a complex soil structure based on geometric coordinate transformation," *IEEE Trans. Power Del.*, vol. 31, no. 1, pp. 96–102, Feb. 2016.

MAOHENG JING received the B.S. degree in electrical and electronic engineering from the University of Huddersfield, U.K., in 2014, and the M.S. degree in electrical power engineering from Newcastle University, U.K., in 2015. He is currently pursuing the Ph.D. degree in electrical engineering from Wuhan University, Wuhan, China. His research interests include the grounding technology and numerical analysis.

XISHAN WEN was born in Xiantao, Hubei, China, in 1962. He received the B.S. degree in electrical engineering from Xi'an Jiaotong University, Xian, China, in 1982, and the M.S. and Ph.D. degrees in high voltage and insulation technology from the Wuhan University of Hydraulic and Electrical Engineering, Wuhan, China, in 1989. From 1989 to 1991, he was a Lecture with the Wuhan University of Hydraulic and Electrical Engineering. He has been a Professor with the Wuhan University of Hydraulic and Electrical Engineering (this university has been recombined with other colleges and renamed Wuhan University, since 2000), since 1995. He is the author of several books, more than 200 articles, and more than 70 inventions. His research interests include researching and teaching of power system overvoltage, high voltage insulation and lightning protection, and grounding technology. He is a member of the National Lightning Protection Standardization Committee and National Electric Power Standardization Committee, China. He is currently an Associate Editor of the journal *High Voltage Engineering*.

HANSHENG CAI received the B.S. degree in electrical engineering and automation from Tianjin University, Tianjin, China, in 1983, and the M.S. degree in high voltage and insulation technology from the Wuhan University of Hydraulic and Electrical Engineering, Wuhan, China, in 1989. He is currently a Senior Engineer at the professor level with the State Key Laboratory of HVDC Transmissions Technology, CSG, China. His current research interests include power system analysis, overvoltage and insulation coordination, lightning protection and grounding technology, and high voltage measurement technology in power systems.

YUN TENG received the B.S. and M.S. degrees in electrical engineering from Wuhan University, Wuhan, China, in 2013, where she is currently pursuing the Ph.D. degree in electrical engineering. Her research interests include power system control, lightning protection, and grounding technology. From 2013 to 2015, she was an Editor in the China Electric Power Press, Beijing, China.

SHANGMAO HU received the M.S. and Ph.D. degrees in electrical engineering from Xi'an Jiaotong University, in 2008 and 2012, respectively, Xi'an, China. He is currently with the State Key Laboratory of HVDC Transmissions Technology, CSG, China. His current research interests include the electrode technology of HVDC, overvoltage, and protection of power systems.

YI ZHANG received the B.Sc. degree in electrical engineering and automation and the Ph.D. degree from Wuhan University, Wuhan, China, in 2006 and 2015, respectively. He is currently with the State Key Laboratory of HVDC Transmissions Technology, CSG, China. His current research interests include lightning protection and grounding technology, and high-voltage measurement technology in power systems.

LEI LAN was born in Zigong, Sichuan, China, in 1969. She received the B.S. degree in information and control engineering from Shanghai Jiao Tong University, Shanghai, in 1991, the M.S. degree in electrical engineering from Sichuan University, Chengdu, in 1997, and the Ph.D. degree in electrical engineering from Wuhan University, Wuhan, in 2004. From 2004 to 2009, she was an Associate Professor, and since 2009, she has been a Professor with Wuhan University. From 2007 to 2008, she was a Visiting Scholar with Arizona State University, USA. She is the author of more than 80 articles. Her research interests include lightning protection, external insulation under contamination condition, and insulating material. Prof. Lan was a recipient of the Science and Technology Progress Award of Hubei Province in China the first prize and the third prize once each.

HAILIANG LU (Member, IEEE) was born in Hubei, China, in 1982. He received the B.S. degree in electrical engineering and its automation and the Ph.D. degree in high voltage and insulation from Wuhan University, Wuhan, China, in 2004 and 2010, respectively. From 2010 to 2017, he was a Lecturer with Wuhan University. During that period, he worked as a Visiting Scholar with The University of Tennessee Knoxville. He is currently an Associate Professor with Wuhan University. He is the author of one book, more than 70 articles, and more than 30 inventions. His research interests include electro-magnetic transient simulation, overvoltage protection, and grounding technology. Dr. Lu is a committee member of IEEE Power & Energy Society and IEEE High Voltage Testing Techniques subcommittee. He currently serves as a working group Member of IEEE P510, IEEE P1122, IEEE P4, and IEEE P2426.